

# **9 Introduction to Full Configuration Interaction Quantum Monte Carlo with Applications to the Hubbard model**

Ali Alavi

Max-Planck-Institut für Festkörperforschung, Stuttgart  
University Chemical Laboratory, Cambridge

## **Contents**

<b>1</b>	<b>Introduction</b>	<b>2</b>
<b>2</b>	<b>FCIQMC</b>	<b>3</b>
<b>3</b>	<b>Semi-stochastic FCIQMC</b>	<b>5</b>
<b>4</b>	<b>Choosing the deterministic space</b>	<b>7</b>
<b>5</b>	<b>An application of FCIQMC to the Hubbard model</b>	<b>8</b>
<b>6</b>	<b>Future perspectives</b>	<b>12</b>

# 1 Introduction

The Full Configuration Interaction Quantum Monte Carlo (FCIQMC) technique is a stochastic method to compute the ground-state energy (and expectation values over two-particle operators of the ground state) of extremely large many-body Hamiltonians, usually in the context of ‘Full CI’ methods: that is to say electronic wavefunctions expanded in Slater determinant spaces comprising of all possible determinants constructable from a given spatial orbital basis. Introduced in 2009 [1], it has been developed in a number of ways which greatly extends the scope of the methodology: the *initiator method* [2], introduced in 2010, enables much larger Hilbert spaces to be accessed with a relatively small number of walkers, albeit at the cost of a systematically improveable bias, followed in 2012 the development of the *semi-stochastic* FCIQMC method (S-FCIQMC) [3,4], which greatly reduces the stochastic error bars for a given amount of computer effort, resulting in  $\sim 1000$ -fold increase in efficiency. In 2014, the *replica method* to compute reduced-density matrices (1- and 2-body) was introduced [5], which has enabled other developments, including property calculations [6], stochastic CASSCF [6,7], and F12 corrections [8], and finally the method was extended to excited states [9–13]. FCIQMC has also led to stochastic techniques for solving other types of quantum chemical equations: the Coupled-Cluster Monte Carlo technique [14], and the density matrix QMC method [15], respectively.

The scope of this short tutorial lecture cannot possibly cover all of the above aspects. We will limit ourselves to the description of the algorithm, together with its semi-stochastic variant, as well as some illustrative examples using the Hubbard model. It should be pointed out, however, that the FCIQMC has proven most useful for quantum chemical systems, often characterized by large basis sets (i.e., a large ratio of the number of orbitals to the number of electrons), and in which the full CI eigenvector is very sparse in comparison to the size of the Hilbert space. FCIQMC manages to perform an efficient sampling of such sparse solutions without *a priori* knowledge of the wavefunction, and importantly, without encountering a severe sign problem. In other words, the signal-to-noise ratio of the simulations are perfectly stable and manageable, and does not deteriorate with time as the simulation proceeds. However, where sparsity does not exist in the wavefunction, in other words where the entire Hilbert space is relevant to the description of the wavefunction, it is inevitable that the computational effort of the FCIQMC simulation involves sampling the whole (exponentially large) space. This is found to be the case for the Hubbard model, where, depending on the strength of the Hubbard  $U$ , the exact solution can be either sparse or dense, the latter being the case for example in the Hubbard model as  $U/t$  becomes large (in a plane-wave basis). In this case, FCIQMC is not much more efficient than conventional exact diagonalization. It does raise the question of representation, though. At very large  $U$  (which by numerical experimentation is found to be around  $30t$ ) it is more efficient to use a real-space representation to express the FCI solution, whereas at smaller  $U$  plane-waves are more efficient. However for the intermediate  $U$  regime, i.e., from 4-12, we have not found any representation to be efficient, and the FCI solution appears to be quite dense in both real and reciprocal space.

Nevertheless, the important property of the FCIQMC method rests on its intrinsic ability to locate the important parts of the wavefunction, *and to entangle them correctly*. In other words the correct linear combination of Slater determinants emerges from the simulation, without the need to perform any explicit diagonalization, or similar numerical procedure. In order to do this, the key step is the *walker-annihilation* step of the algorithm, which will be discussed later on. It turns out that this process can be done in a *local* manner, in an  $\mathcal{O}(N_w)$  process, i.e., scaling linearly with the number of walkers, without the need to invoke global processes involving the entire walker population or Hilbert space, which would be intractable. Furthermore, this allows for massive parallelization, which is without doubt one of the key strengths of the technique. It gives it an exciting future perspective.

## 2 FCIQMC

Given a second-quantized Hamiltonian of the type

$$\hat{H} = \sum_{pq} h_{pq} c_p^\dagger c_q + \sum_{pqrs} v_{pqrs} c_p^\dagger c_q^\dagger c_s c_r \quad (1)$$

defined over a set of spin-orbitals  $\{\varphi_1, \dots, \varphi_p, \dots, \varphi_q, \dots, \varphi_{2M}\}$  with

$$h_{pq} = \langle \varphi_p | h | \varphi_q \rangle \quad (2)$$

$$v_{pqrs} = \langle \varphi_p \varphi_q | r_{12}^{-1} | \varphi_r \varphi_s \rangle, \quad (3)$$

the object is to solve for the lowest-energy eigenstate of such an Hamiltonian for an  $N$ -electron system

$$\hat{H} |\Psi_0\rangle = E_0 |\Psi_0\rangle. \quad (4)$$

FCIQMC can be considered as a stochastic minimization of the energy with respect to a sampled full configuration interaction wavefunction expansion. This wavefunction is a simple linear combination of all Slater determinants that can be constructed from distributing the available electrons within the (orthonormalized) single-particle orbitals spanning the space, as

$$|\Psi_0\rangle = \sum_{\mathbf{i}} C_{\mathbf{i}} |D_{\mathbf{i}}\rangle, \quad (5)$$

where  $|D_{\mathbf{i}}\rangle$  represents a Slater determinant, labeled by the orbital-occupation string  $\mathbf{i}$ . The linear coefficients of this expansion are the objects that are stochastically sampled using a *delta function* or *walker* representation: given an ensemble of  $N_w$  walkers distributed over the Hilbert space, each with a sign  $s = \pm 1$  and Slater determinant  $\mathbf{i}$

$$\{s_1 \mathbf{i}_1, s_2 \mathbf{i}_2, \dots, s_{N_w} \mathbf{i}_{N_w}\} \quad (6)$$

the number of walkers on each determinant is

$$n_{\mathbf{i}} = \sum_w^{N_w} s_w \delta(\mathbf{i}_w - \mathbf{i}). \quad (7)$$

The FCIQMC algorithm is then a population dynamics of such an assembly of walkers with the aim that in a long-time ( $\beta$ ) simulation, the expectation value of the  $n_i$  becomes proportional to the  $C_i$

$$\langle n_i \rangle_\beta \propto C_i. \quad (8)$$

The stochastic, iterative equations that govern this dynamics are given by

$$\Delta n_i(\beta + \tau) = -\tau \left[ \sum_{j \neq i} H_{ij} n_j(\beta) \right] - \tau(H_{ii} - S) n_i(\beta), \quad (9)$$

where  $\Delta n_i(\beta)$  represents the change in ‘walker’ population/weight on determinant  $|D_i\rangle$  in the time step  $\beta \rightarrow \beta + \tau$ . This leads to population dynamics of a set of walkers which occupy determinants connected to each other in this many-electron Hilbert space. This dynamics can be achieved by a set of local, stochastically realized, Markov-chain processes as follows:

The first is a ‘spawning’ step, which is performed for each occupied determinant, and a number of times proportional to the walker weight at that determinant ( $n_i$ ). A single or double excitation is randomly chosen, with normalized probability  $p_{\text{gen}}(\mathbf{j}|\mathbf{i})$  for the excitation from  $|D_i\rangle$  to  $|D_j\rangle$ . The walker amplitude on  $|D_j\rangle$  is then augmented with a signed probability given by

$$p_{\text{spawn}} = -\frac{\tau H_{ij}}{p_{\text{gen}}(\mathbf{j}|\mathbf{i})}. \quad (10)$$

Finally, a ‘death’ step is performed, by which the amplitude on each determinant,  $|D_i\rangle$ , is (generally) reduced with probability  $\tau(H_{ii} - S)n_i$ . Taken together, these two steps simulate the dynamic in Eq. (9). However, an additional ‘annihilation’ step is essential in order to overcome an exponential increase in noise and other features associated with the Fermion sign problem [1]. In this step, walkers of opposite signs on the same determinant are removed from the simulation.

The energy of the QMC-sampled wavefunction can be extracted from a projected estimator, the simplest of which is

$$E_{\text{Proj}} = \frac{\langle D_{\text{HF}} | \hat{H} | \Psi \rangle}{\langle D_{\text{HF}} | \Psi \rangle}, \quad (11)$$

where the projection is done onto the Hartree-Fock determinant  $D_{\text{HF}}$ . This is a reasonable projection as long as  $D_{\text{HF}}$  has a non-negligible overlap with the ground-state wavefunction  $\Psi$ . In case of wavefunctions with multi-reference character, it is better to perform a projection onto a multi-determinantal trial wavefunction  $\Psi_T = \sum_{\{\mathbf{i}\}} C_{\mathbf{i}}^T |D_{\mathbf{i}}\rangle$ , so that

$$E_T = \frac{\langle \Psi_T | \hat{H} | \Psi \rangle}{\langle \Psi_T | \Psi \rangle}. \quad (12)$$

For a well-chosen  $\Psi_T$ , so that the denominator stays far from zero (which can be generated on the fly during the FCIQMC simulation), this leads to a significantly better behaved energy

estimator with smaller bias and smaller stochastic errors. In the NECI code,  $\Psi_T$  is generated by diagonalizing  $H$  in a sub-space containing a specified number of leading determinants obtained from an FCIQMC simulation.

The value of the shift  $S$  is varied throughout the simulation in order to maintain a constant, desired weight of walkers. At convergence, this value should fluctuate about the energy of the system, providing an alternative estimator for the energy based on the total growth rate of all the walkers in the system. More details on the specific implementation of these steps, and the derivation of this dynamic from the imaginary-time Schrödinger equation can be found in Refs. [1, 16, 3]. Furthermore, the systematically improvable *initiator* approximation is almost always used (sometimes denoted *i*-FCIQMC to distinguish it from the full method). This involves a dynamically truncated Hamiltonian operator, where spawning events to unoccupied determinants are constrained to be only allowed if they come from a determinant with a walker weight greater than  $n_{\text{add}}$ . This approximation can be systematically improved as the number of walkers increases, as increasing numbers of determinants fulfil the criteria, and the sampled Hamiltonian therefore approaches the exact Hamiltonian. More details and benchmarking of this approximation can be found in Refs. [2, 17].

### 3 Semi-stochastic FCIQMC

The FCIQMC wave function is represented by a collection of walkers which have a weight and a sign and reside on a particular basis state, sometimes referred to as a *site*. The total signed weight of walkers on a site is interpreted as the amplitude of that basis state in the (unnormalized) FCI wave function expansion. The FCIQMC algorithm consists of repeated application of the projection operator

$$\hat{P} = \mathbb{1} - \tau(\hat{H} - S\mathbb{1}) \quad (13)$$

to some initial state, where  $\hat{H}$  is the Hamiltonian operator,  $\tau$  is some small time step and  $S$  is an energy offset (‘shift’) applied to the Hamiltonian to control the total walker population. With sufficiently small  $\tau$ , exact repeated application of  $\hat{P}$  will project the initial state to the ground state of  $\hat{H}$  [18]. In FCIQMC,  $\hat{P}$  is applied such that the correct projection is only performed on average, thus leading to a stochastic sampling of the ground state wave function.

The projection operator can be expanded in the chosen FCI basis as

$$\hat{P} = \sum_{\mathbf{ij}} P_{\mathbf{ij}} |\mathbf{i}\rangle \langle \mathbf{j}|. \quad (14)$$

In the semi-stochastic adaptation the set of basis states is divided into two sets,  $D$  and  $S$ . We refer to the space spanned by those basis states in  $D$  as the *deterministic space*, and refer to the basis states themselves as *deterministic states*. The terms in Eq. (14) can then be divided into two separate operators,

$$\hat{P} = \hat{P}^D + \hat{P}^S, \quad (15)$$

where  $\hat{P}^D$  refers to the deterministic projection operator,

$$\hat{P}^D = \sum_{i \in D, j \in D} P_{ij} |\mathbf{i}\rangle \langle \mathbf{j}|, \quad (16)$$

and  $\hat{P}^S$  is the stochastic projection operator containing all other terms. In semi-stochastic FCIQMC,  $\hat{P}^D$  is applied exactly by performing an exact matrix multiplication, while  $\hat{P}^S$  is applied using the stochastic FCIQMC spawning steps as usual.<sup>1</sup>

In order to perform an exact projection in the deterministic space, the walkers weights must be allowed to be non-integers. This differs from most previous descriptions of the FCIQMC algorithm thus far. To be clear in notation, we use  $C_i$  to refer to the *signed* amplitude on a site, and  $N_i$  to refer to the *unsigned* amplitude (and so  $|C_i| = N_i$ ), which we refer to as the *weight* on the site.

A complete iteration of semi-stochastic FCIQMC is performed as follows, where we use the notation  $\hat{T} = -(\hat{H} - S\mathbb{1})$ :

1. **stochastic projection:** Loop over all sites. Perform  $\chi_i$  spawning attempts from site  $|\mathbf{i}\rangle$ , where  $\chi_i$  is specified below. For each spawning attempt, choose a random connected site  $|\mathbf{j}\rangle$  with probability  $p_{ij}$ , where connected means that  $H_{ij} = \langle \mathbf{i} | H | \mathbf{j} \rangle \neq 0$  and  $\mathbf{i} \neq \mathbf{j}$ . The attempt fails if both  $|\mathbf{i}\rangle$  and  $|\mathbf{j}\rangle$  belong to  $D$ , otherwise a new walker on site  $|\mathbf{j}\rangle$  is created with weight  $|T_{ji}| \text{sign}(C_i) \tau / p_{ij}$ .
2. **deterministic projection:** New walkers are created on sites in  $D$  with weights equal to  $\tau \mathbf{T}^D \mathbf{C}^D$ , where  $\mathbf{C}^D$  is the vector of amplitudes currently on sites in  $D$ .
3. **death/cloning:** Loop over all sites in  $S$ . For each site create a spawned walker with weight and sign given by  $T_{ii} C_i \tau$ .
4. **annihilation:** Combine all newly spawned walkers with walkers previously in the simulation by summing together the weights of all walkers on the same site.

$\chi_i$  is chosen probabilistically such that the expectation value  $E[\chi_i] = N_i$ . Although other approaches have been used [3], in this work we set

$$\chi_i = \lceil N_i \rceil \quad \text{with probability } N_i - \lfloor N_i \rfloor, \quad (17)$$

$$= \lfloor N_i \rfloor \quad \text{otherwise.} \quad (18)$$

If integer weights are used, then this reduces to  $\chi_i = N_i$ , as used in previous work [1].

In order to reduce the memory demands of having a large number of sites occupied with a low weight, a minimum occupation threshold,  $N_{\text{occ}}$ , is defined. After all annihilation has occurred, any walkers with a weight less than  $N_{\text{occ}}$  are rounded up to  $N_{\text{occ}}$  with probability  $N_i/N_{\text{occ}}$  or otherwise down to 0. In practice, we always choose  $N_{\text{occ}} = 1$ . The occupation threshold is not applied to deterministic states such that the deterministic projection is applied exactly.

<sup>1</sup>If the deterministic space is the entire FCI space, then the algorithm reduces to the power method without explicit normalization; FCIQMC can be viewed as a stochastic version of this approach.

We further use a modification to the initiator adaptation to FCIQMC [2, 19] by allowing all spawnings both from and to the deterministic space to survive. This effectively forces all deterministic states to be initiators, which is sensible since these states should be selected by their importance (i.e. weight). We note that this is different from the more complicated adaptation made by Petruzielo *et al.* [3], where the initiator threshold is allowed to vary based on the number of steps since a walker last visited the deterministic space. We note that it is not necessary to use both the initiator and semi-stochastic adaptations together; the benefits from both extensions are largely independent of each other.

Using non-integer weights can have a significant memory impact compared to integer weights due to the large number of additional spawned walkers, which also increases time demands due to expensive extra processing and communication steps. We therefore apply an unbiased procedure to stochastically remove walkers with very small weights, similar to that above. Following the notation of Overy *et al.* [5], we use a spawning cutoff,  $\kappa$ , where  $\kappa = 0.01$  unless stated otherwise. A spawning of weight  $N_j < \kappa$  is rounded up to  $\kappa$  with probability  $N_j/\kappa$  or otherwise down to 0. Spawned walkers with weights greater than  $\kappa$  are left unaltered.

## 4 Choosing the deterministic space

The key to reducing the stochastic error is to choose  $D$  such that most of the weight of the true FCI wave function is in this space. For a given number of basis states in the deterministic space,  $|D|$ , it is expected that the best possible deterministic space (the one which reduces noise the most) is obtained by choosing the  $|D|$  most highly weighted basis states in the exact expansion of the ground-state wave function. Achieving this optimal space requires knowledge of the exact wave function and so is not feasible in general.

A sensible choice for  $D$  in many systems would be a configuration interaction (CI) or complete active space (CAS), generally regarded as being effective at describing situations where dynamical and static correlation, respectively, are important. We have found from experience that such spaces are useful and lead to a large reduction in stochastic noise. This leads to the question: can one find a better deterministic space, at least in common cases?

Petruzielo *et al.* [3] describe an iterative method for choosing the deterministic space. First the space connected to the space from the previous iteration is generated and the ground state of the Hamiltonian in this subspace is calculated. The most significant basis states in this ground-state expansion are kept (according to a criterion on the amplitude of coefficients). The initial space contains (e.g.) the Hartree–Fock determinant. This process is repeated for some number of iterations. This approach has been demonstrated to give much greater improvements than by simply using the space connected to the Hartree–Fock state, even with a reduced size for  $D$ , as it can contain the chemically-relevant basis states [3].

In the NECI code we use a different method of generating the deterministic space. Inspired by the spirit of FCIQMC, we allow the deterministic space to emerge from the calculation itself: we simply perform a fully-stochastic FCIQMC calculation (or a semi-stochastic calculation with a simple deterministic space, such as a CISD space) until the ground state is deemed to have

been reached, and then choose the most populated basis states in the FCIQMC wave function to form  $D$ . In this initial FCIQMC calculation, it is not necessary to employ a large number of walkers, as its purpose is simply to identify determinants which are likely to be important in the converged solution. The generation of the deterministic subspace is therefore extremely rapid. This approach has the benefit that it does not require performing an exact ground-state diagonalization within a (potentially large) subspace, which can be very expensive. The only parameter is the desired size of the deterministic space and it is therefore considerably more black-box like. Since the initial FCIQMC calculation need not be limited to low-order excitations (such as the double excitations of a reference determinant), but can develop significant walker population on some determinants deep in the Hilbert space (on quadruple, sextuple and higher excitation levels) our procedure can select close-to-optimal deterministic spaces in a very inexpensive and rapid manner.

Although the FCIQMC wave function is only a stochastic snapshot of the true ground state, the most significant basis states in the expansion will tend to remain highly occupied throughout the simulation with weights fluctuating about their exact values. It is therefore not surprising that our approach works well. For very large deterministic spaces, states with the minimum occupation weight, may be included in the space. In this case there is some redundancy in how  $D$  is chosen, and the choice of  $D$  will probably not be optimized fully, although we still find this approach to work very well. It is simple to include a cutoff to avoid this if desired, although we do not do so in the calculations presented here.

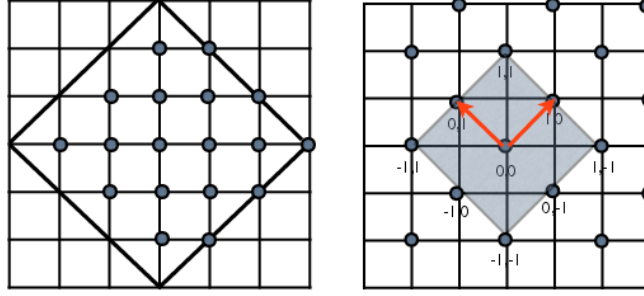
We emphasize that we prefer our approach to the iterative scheme of Petruzielo *et al.* because it avoids large ground-state calculations which, for large systems and values of  $|D|$ , can take up a significant amount of time and memory. If the size of the space at the start of an iteration in this iterative scheme is given by  $X$ , and the average number of connections to each state is  $n_c$  (which, in general, grows quadratically with system size), then one will have to perform a ground-state calculation in a space of size  $\sim Xn_c$ . For many cases, including those considered in this article, such a space is extremely, if not prohibitively, large. Indeed, as FCIQMC is applied to increasingly larger systems, such an approach will become less feasible. Already, FCIQMC has been applied to systems where the number of connections to the Hartree–Fock state is  $\mathcal{O}[10^5 - 10^6]$  [20, 6]. In these cases, it might be possible to apply the iterative scheme if only a small number of states are kept in each iteration, but in this case the final space would be unoptimized. Another approach would be to generate the final space by finding the connections to the previous (small) space but *not* performing a ground-state calculation, but again the generated space would be unoptimized. We therefore feel that our approach is an altogether more black box and scalable approach to generating an effective deterministic space.

## 5 An application of FCIQMC to the Hubbard model

The Hubbard model Hamiltonian is usually expressed in a real-space lattice as

$$\hat{H} = -t \sum_{\langle p,q \rangle, \sigma} (c_{p\sigma}^\dagger c_{q\sigma} + \text{h.c.}) + U \sum_p n_{p\uparrow} n_{p\downarrow}, \quad (19)$$

$3\sqrt{2} \times 3\sqrt{2}$ , 18 sites ( $L=3$ )



$$\begin{aligned} \mathbf{T}_1 &= (L, L) \\ \mathbf{T}_2 &= (-L, L) \end{aligned}$$

$$\begin{aligned} \mathbf{b}_1 &= \frac{\pi}{L}(1, 1) \\ \mathbf{b}_2 &= \frac{\pi}{L}(-1, 1) \end{aligned}$$

**Fig. 1:** The 18-site Hubbard model on a tilted lattice. (a) Real-space lattice. (b) Reciprocal space lattice, showing the occied Fermi ‘square’ at half-filled occupancy

where  $n_{p\sigma} = c_{p\sigma}^\dagger c_{p\sigma}$  is the number operator on site  $p$  for  $\sigma$ -spin electrons. The sum  $\langle p, q \rangle$  is taken over nearest-neighbor lattice sites  $p$  and  $q$  and periodic boundary conditions are applied. Twisted periodic boundary conditions can also be applied, in order to reduce finite size effects and to perform “twist-averaging”, but in the numerical examples below this is not done. For the purposes of FCIQMC, it is more convenient to work in a plane-wave, reciprocal space, representation in which the orbitals are unitarily transformed as

$$|\mathbf{k}\rangle = \frac{1}{\sqrt{\Omega}} \sum_p e^{-i\mathbf{k}\cdot\mathbf{r}_p} |p\rangle, \quad (20)$$

where  $\Omega$  is the number of sites in the lattice and  $\mathbf{r}_p$  is the position of lattice site  $p$ . In this momentum basis, the Hubbard Hamiltonian takes the form

$$\hat{H} = \sum_{\mathbf{k}, \sigma} \epsilon_{\mathbf{k}} c_{\mathbf{k}, \sigma}^\dagger c_{\mathbf{k}, \sigma} + \frac{U}{\Omega} \sum_{\mathbf{k}, \mathbf{q}, \mathbf{Q}} c_{\mathbf{k}+\mathbf{Q}, \uparrow}^\dagger c_{\mathbf{q}-\mathbf{Q}, \downarrow}^\dagger c_{\mathbf{k}\uparrow} c_{\mathbf{q}\downarrow}. \quad (21)$$

The precise form of  $\epsilon_{\mathbf{k}}$  depends on the lattice vectors of the lattice being studied. For this study we shall use the tilted 2-dimensional square lattice shown in Fig. 1, with super-cell lattice vectors

$$\mathbf{T}_1 = \begin{pmatrix} L \\ L \end{pmatrix} \quad \text{and} \quad \mathbf{T}_2 = \begin{pmatrix} -L \\ L \end{pmatrix}, \quad (22)$$

where  $L$  is an odd integer. This leads to a supercell containing  $\Omega = \sqrt{2}L \times \sqrt{2}L$  sites. The dispersion relation for  $\epsilon_{\mathbf{k}}$  can be expressed in terms of the reciprocal lattice vectors of  $\mathbf{T}_1, \mathbf{T}_2$ , namely  $\mathbf{b}_1, \mathbf{b}_2$

$$\mathbf{b}_1 = \frac{\pi}{L} \begin{pmatrix} 1 \\ 1 \end{pmatrix} \quad \text{and} \quad \mathbf{b}_2 = \frac{\pi}{L} \begin{pmatrix} 1 \\ -1 \end{pmatrix} \quad (23)$$

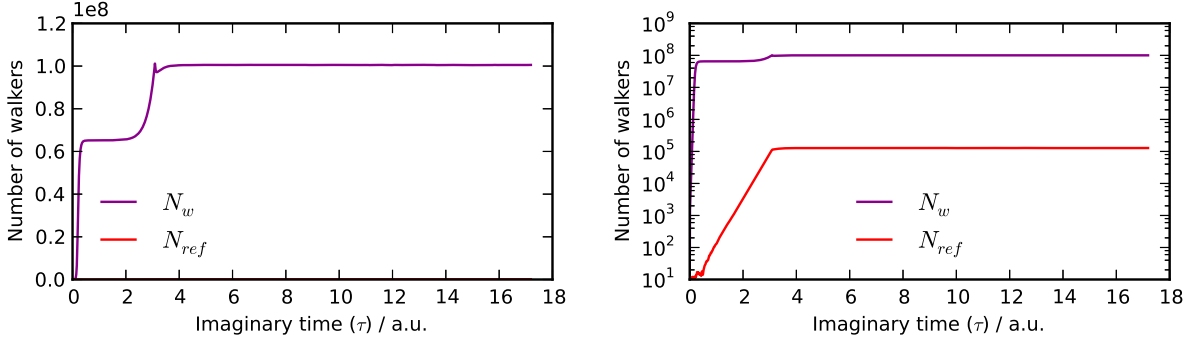


**Fig. 2:** The number of walkers in a non-initiator FCIQMC calculation, showing a plateau for the  $(18,18)$   $U/t = 4$  system at  $\approx 62 \times 10^6$  walkers. The second plateau corresponds to the onset of variable-shift mode, in which the walker population is stabilized at  $10^8$  walkers. The Hilbert space corresponds to  $\approx 131 \times 10^6$  determinants. The number of walkers on the reference determinant is 127000, and is barely visible on this plot. The plot on the right shows the same information on a logarithmic scale.

with allowable  $\mathbf{k} = \mathbf{k}_{n,m}$  as follows:

$$\mathbf{k}_{n,m} = n\mathbf{b}_1 + m\mathbf{b}_2 \quad (24)$$

$$\epsilon_{\mathbf{k}} = -2t \left( \cos \frac{\pi(n+m)}{L} + \cos \frac{\pi(n-m)}{L} \right) \quad (25)$$

We are aware of exact diagonalization results for the half-filled 18-site ( $L = 3$ ) model to which we will compare the FCIQMC results [21], which we shall refer to as the  $(18, 18)$  system. This system has a Hilbert space of  $N_{FCI} \approx \frac{1}{18} \binom{18}{9}^2 \approx 131 \times 10^6$  Slater determinants. The calculations have been done with  $\tau = 0.001$  for a range of  $U/t = 1 - 4$ . We have also performed calculations on the Hubbard model with 2 holes (maintaining zero momentum and zero total spin), i.e., the  $(18, 16)$  system, to exhibit the effect of moving off half-filling on the FCIQMC method.

We first perform a non-initiator FCIQMC calculation, which exhibits a *plateau* in the walker growth when the shift is held fixed at  $S = 0$  (Fig. 2). This plateau occurs when roughly 50% of the Hilbert space has been populated by walkers. For smaller values of  $U$ , the plateau height decreases linearly, vanishing when  $U < 1$  (Fig. 3). This implies that for such values of  $U$ , it is possible to sample the Hilbert space with a vanishingly small number of walkers [22] even without the initiator method.

Figure 4 shows the error in the projected energy as a function of imaginary time for the  $(18,18)$  Hubbard model with  $U/t = 4$  using FCIQMC without the initiator method. With the initiator method, it can be seen that a small but systematic bias is induced at small walker population, which diminishes with increasing number of walkers. Even with a small number of walkers, the simulations are stable with a constant signal to noise ratio in the long time limit. This is shown in Fig. 5 for the  $(18,18)$  and the  $(18,16)$  Hubbard model, both with  $U/t = 4$ . The cost of the initiator runs is however much lower. Fig. 6 shows the time per iteration for each of the runs, including the  $10^8$  walker non-initiator run. The time per iteration is linear in the number of walkers, and there additional overhead associated with the initiator method compared to the full method.

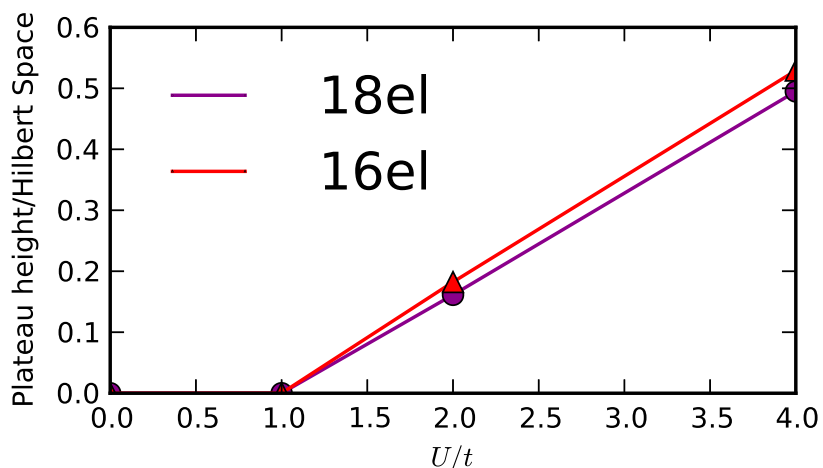


**Fig. 3:** The ratio of plateau heights to the size of the Hilbert space as a function of  $U$  for the 18-electron and 16-electron (2-hole) system. As the value of  $U$  decreases, an off-set linear decrease in the plateau height is observed, vanishing at  $U = 1$ . The 2-hole system exhibits slightly higher values of the plateau as a ratio of the Hilbert space, presumably because of the more multi-reference nature of the ground state wavefunction.

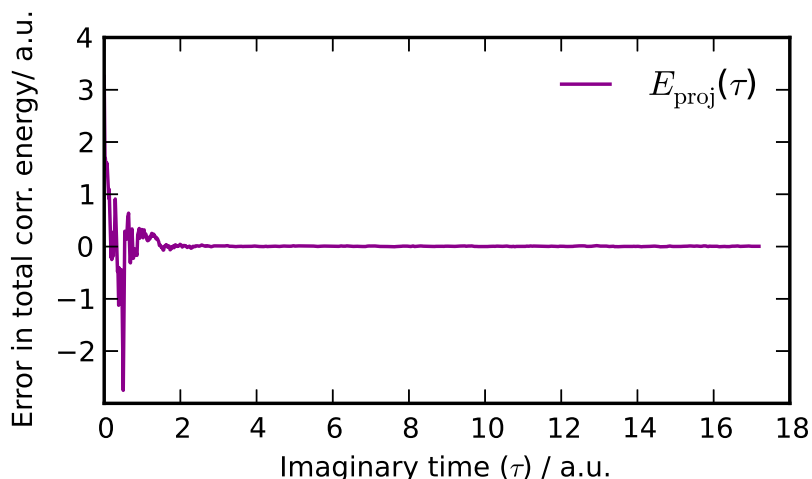


**Fig. 4:** The error in the projected energy as a function of imaginary time for the (18,18) Hubbard model at  $U/t = 4$ . The initiator method is not used, leading to a plateau in the walker-growth of the simulation (see Fig. 2). The initial value of the energy is the Hartree-Fock energy ( $-14t$ ), which is  $3.25239t$  above the exact energy of  $-17.25239t$ . All energy plots are shown relative to this exact energy. It is evident that after propagation of  $\approx 2$  units of imaginary time ( $\tau = 0.001t$ ), the simulation has converged, and crucially, the energy stable, i.e., there is no growth in noise as the simulation proceeds.

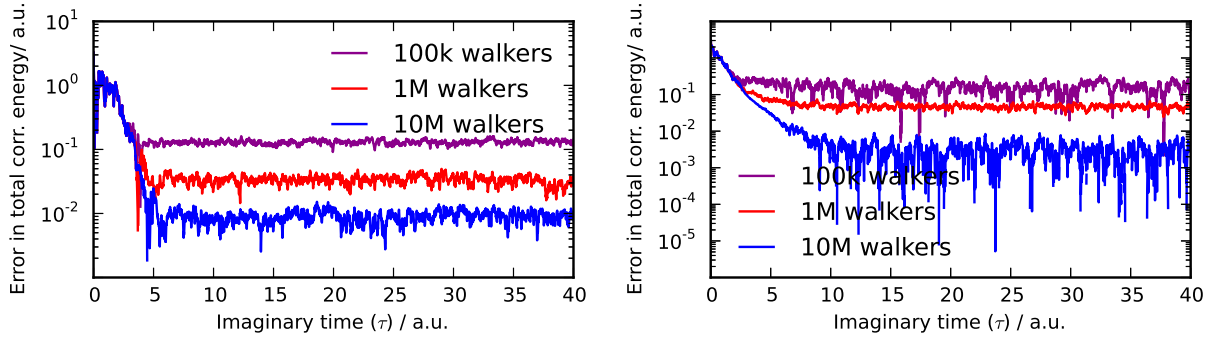


**Fig. 5:** Error of different initiator runs of varying number of walkers for the Hubbard model with  $U/t = 4$ . Left: Half-filled (18,18) system. The initiator error is seen to decrease as the walker population is increased. The signal to noise ratio of the initiator simulations is also stable in the long time limit, even with low walker population. Right: 2-hole doped (18,16) system. The behavior is very similar to the half-filled case, indicating that the severity of the sign-problem is not increased when moving away from half-filling. Indeed the convergence of the initiator bias is faster, owing presumably to the smaller Hilbert space of the 2-h system.

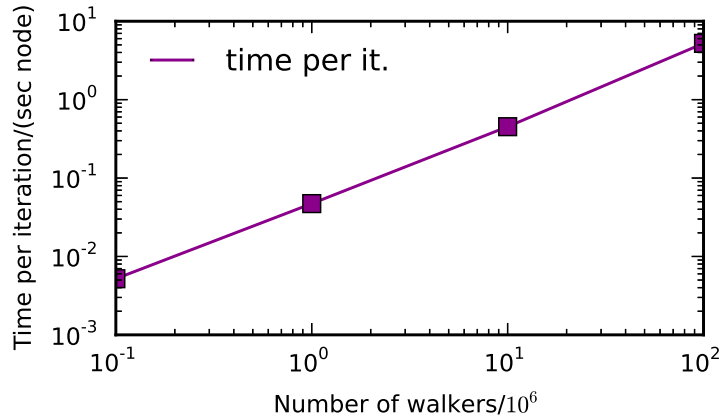


**Fig. 6:** Time per iteration on one node (20 core) as a function of the number of walkers. The three runs at 100k, 1M, and 10M walkers were initiator simulations, whilst the run with  $10^8$  walkers is a non-initiator simulation.

## 6 Future perspectives

Although the FCIQMC technique has thus far been formulated in a Slater determinant basis, its ideas can be extended to other more general types of basis functions which span the same Hilbert space. A notable example are configuration state functions (CSFs), each one of which preserves the total spin  $S$  quantum number, in addition to the spin-polarization quantum number  $M_S$ . Spaces of CSFs are typically an order of magnitude smaller than the corresponding Slater determinant basis, but the matrix element calculations between CSFs is more complex. Development of fast algorithms capable of handling CSFs would greatly help in the study of systems with small spin-gaps (which includes Hubbard models in the intermediate  $U$  range), and we believe this to be an important area of research. Another important question is to understand the factors that govern the rate of convergence of the initiator method, with the aim to

try to improve it. In the study of quantum chemical systems, and of the uniform electron gas, it is frequently found that the initiator method works extremely well, so that Hilbert spaces as large as  $10^{108}$  have been sampled with  $\sim 10^9$  walkers [23]. However for the 2D Hubbard model, particularly in the ‘interesting’ range of  $U/t = 4 - 12$  one observes much larger initiator biases. Is this inevitable? In other words, is the complexity of the ground-state wavefunction such that, no matter which technique is employed, the convergence is governed by the complete Hilbert space? This is unclear. Perhaps some fusion of FCIQMC with other types of wavefunction representations, such as matrix product states or tensor networks could be envisaged. But there is at present no equivalent projector method to FCIQMC in such representations which does so – only variational methods or fixed-node approximations. These are indeed extremely important questions to be addressed in the future.

## Acknowledgments

I am grateful to a large number of former and present PhD students and postdocs who have helped develop the FCIQMC method and the NECI code, in Cambridge and in Stuttgart: George Booth, Alex Thom, Diedre Cleland, Simon Smart, James Shepherd, Nick Blunt, Catherine Overy, Jennifer Kersten, Robert Thomas, Werner Dobrazt, Giovanni Li Manni, Sasha Lozovoi, Dongxia Ma, Guillaume Jeanmairet, and Michele Ruggeri. The work has been funded by the EPSRC and by the Max Planck Society.

## References

- [1] G.H. Booth, A.J.W. Thom, and A. Alavi, *J. Chem. Phys.* **131**, 054106 (2009)
- [2] D.M. Cleland, G.H. Booth, and A. Alavi, *J. Chem. Phys.* **132**, 041103 (2010)
- [3] F.R. Petruzielo, A.A. Holmes, H.J. Changlani, M.P. Nightingale, and C.J. Umrigar, *Phys. Rev. Lett.* **109**, 230201 (2012)
- [4] N.S. Blunt, S.D. Smart, J.A.F. Kersten, J.S. Spencer, G.H. Booth, and A. Alavi, *J. Chem. Phys.* **142**, 184107 (2015)
- [5] C. Overy, G.H. Booth, N.S. Blunt, J.J. Shepherd, D. Cleland, and A. Alavi, *J. Chem. Phys.* **141**, 244117 (2014)
- [6] R.E. Thomas, G.H. Booth, and A. Alavi, *Phys. Rev. Lett.* **114**, 033001 (2015)
- [7] G. Li Manni, S. Smart, and A. Alavi, *J. Chem. Theor. Comput.* **12**, 1245 (2016)
- [8] G.H. Booth, D. Cleland, A. Alavi, and D.P. Tew, *J. Chem. Phys.* **137**, 164112 (2012)
- [9] G.H. Booth and G.K.-L. Chan, *J. Chem. Phys.* **137**, 191102 (2012)
- [10] S. Ten-no, *J. Chem. Phys.* **138**, 164126 (2013)
- [11] A. Humeniuk and R. Mitrić, *J. Chem. Phys.* **141**, 194104 (2014)
- [12] N.S. Blunt, A. Alavi, and G.H. Booth, *Phys. Rev. Lett.* **115**, 050603 (2015)
- [13] N.S. Blunt, G.H. Booth, and A. Alavi, *J. Chem. Phys.* **143**, 134117 (2015)
- [14] A. Thom, *Phys. Rev. Lett.* **105**, 263004 (2010)
- [15] N.S. Blunt, T.W. Rogers, J.S. Spencer, and W.M.C. Foulkes, *Phys. Rev. B* **89**, 245124 (2014)
- [16] G.H. Booth, S.D. Smart, and A. Alavi, *Mol. Phys.* **112**, 1855 (2014)
- [17] G.H. Booth, A. Grüneis, G. Kresse, and A. Alavi, *Nature* **493**, 365 (2012)
- [18] J.S. Spencer, N.S. Blunt, and W.M.C. Foulkes, *J. Chem. Phys.* **136**, 054110 (2012)
- [19] D.M. Cleland, G.H. Booth, and A. Alavi, *J. Chem. Phys.* **134**, 024112 (2011)
- [20] J.J. Shepherd, G.H. Booth, and A. Alavi, *J. Chem. Phys.* **136**, 244101 (2012)
- [21] H. Lin, *Phys. Rev. B* **44**, 7151 (1991)
- [22] J.J. Shepherd, G. Scuseria, and J.S. Spencer, *Phys. Rev. B* **90**, 155130 (2014)
- [23] J.J. Shepherd, G.H. Booth, A. Grüneis, and A. Alavi, *Phys. Rev. B* **85**, 081103(R) (2012)